Regulation of Archease by the mTOR-vATPase axis

Deanne Francis*, Alondra S. Burguete[1,‡] and Amin Ghabrial[2,‡,§]

[1]The Motor Neuron Center, Columbia University Medical Center, VP&S 5th floor, New York, NY 10032, USA
[2]Department of Pathology and Cell Biology, Columbia University Medical Center, 630 168th St; Vagellos Physicians and Surgeons 14-401L, New York, NY 10032, USA

*Present address: James Cook University, 1 James Cook Dr, Douglas, QLD, Australia 4811.
‡Co-Senior Authors
§Author for correspondence: amin.ghabrial@gmail.com

SUMMARY STATEMENT

Drosophila Archease is required for apical membrane expansion and its subcellular localization is regulated by TOR-vATPase activity.

Abstract

Larval terminal cells of the *Drosophila* tracheal system generate extensive branched tubes, requiring a huge increase in apical membrane. We discovered that terminal cells compromised for apical membrane expansion – mTOR-vATPase axis and apical polarity mutants – were invaded by the neighboring stalk cell. The invading cell grows and branches, replacing the original single intercellular junction between stalk and terminal cell with multiple intercellular junctions . Here we characterize *disjointed*, a mutation in the same phenotypic class. We find that *disjointed* encodes *Drosophila* Archease, required for RNA ligase (RtcB) function critical for tRNA maturation and ER stress-regulated nonconventional splicing of *Xbp1* mRNA. We show that the steady-state subcellular localization of Archease is principally nuclear, and dependent upon

TOR-vATPase activity. In tracheal cells mutant for *Rheb* or *vATPase*, Archease localization shifted dramatically from nucleus to cytoplasm. Further, we found that blocking tRNA maturation by knockdown of *tRNAse z* also induced compensatory branching. Taken together, these data suggest that the TOR-vATPase axis promotes apical membrane growth in part through nuclear localization of Archease, where Archease is required for tRNA maturation.

INTRODUCTION

The *Drosophila* tracheal system consists of an interconnected network of branched tubes. The system originates from 10 pairs of epithelial sacs composed of roughly 80 cells each. During embryogenesis, these sacs, which have invaginated from the surface epithelium, undergo successive rounds of branching (Ghabrial, Luschnig et al. 2003, Schottenfeld, Song et al. 2010). In primary branching, tip cells actively migrate and pull trailing cells along behind them; in this manner, typical sacs give rise to 6 primary branches(Ribeiro, Neumann et al. 2004, Ghabrial and Krasnow 2006, Caussinus, Colombelli et al. 2008). The largest tubes are multicellular and smaller tubes are autocellular (surrounding a lumenal space and sealing by formation of autocellular junctions) or seamless (elaborating an internal apical membrane that extends through the branches of stellate shaped terminal cells)(Samakovlis, Hacohen et al. 1996). Secondary and tertiary branching are accompanied by specification of “fusion” cells that mediate anastomoses with neighboring branches, and terminal cells extend blind-ended seamless tubes to target tissues(Samakovlis, Manning et al. 1996). Embryonic tracheal terminal cells are the ultimate cells in tracheal branches and are connected to the network via intercellular junctions with their neighboring autocellular stalk cells. Terminal cells initially form a single intracellular blind-ended tube, but subsequently, during larval life, sprout dozens of long, highly-branched “seamless” tubes (Samakovlis, Hacohen et al. 1996, Ghabrial, Luschnig et al. 2003, Schottenfeld, Song et al. 2010). These tubes are initially liquid-filled, but undergo gas-filling at molts (Manning 1993, Tsarouhas, Senti et al. 2007). During each instar, new larger tubes are constructed around the pre-

existing gas-filled tubes, and become gas-filled themselves at the molt. In terminal cells, the new tubes are not only larger, but include new branches targeting additional tissues.

The apical (lumenal) membrane domain of terminal cells must expand dramatically to permit new tubes to ramify adequately on internal tissues, thus permitting gas exchange. Mutations that restrict the generation of apical membrane in terminal cells, such as *v-ATPase* and *Rheb* mutations, or that directly affect the generation of apical polarity, such as *aPKC* and *par6* mutations, cause compensatory growth of the neighboring wild type stalk cells, which lengthen, invade and branch within the mutant terminal cells (Francis and Ghabrial 2015). Mutations in two vATPase genes were isolated based on the presence of a gas-filling defect in what appeared to be the terminal cell tube, adjacent to the position where the intercellular junction connecting terminal (seamless tubes) and stalk (autocellular tube) cells would normally be found. In fact, the tube lacking gas-filling is actually that of the invading stalk cell – the failure to gas-fill may be related to the remodeling that occurs as an autocellular tube replaces the seamless tube, or may reflect the fact that liquid clearance typically occurs during molts and newly made tubes remain liquid filled in-between molts (Manning 1993). Because the autocellular tubes of the stalk cell penetrate dozens of microns into the compromised terminal cell, and branch, the result are pairs of terminal and stalk cells with multiple intercellular junctions marking the connections of stalk cell-derived autocellular tubes – surrounded by terminal cell cytoplasm – and terminal cell-derived seamless tubes.

In a previously described forward genetic screen, we identified mutations in 4 loci that caused related gas-filling defects (Ghabrial, Levi et al. 2011). Upon further characterization, one of these loci, *lotus*, was distinct, preventing the formation of a stable connection between autocellular and seamless tubes (Song, Eng et al. 2013), whereas mutations in the other 3 loci induced compensatory growth from neighboring wild type stalk cells, as described above (Francis and Ghabrial 2015). We identified two of those loci as components of the vATPase (*oak gall*/*Vha26* and *conjoined*/*Vha13*); here we identify the remaining locus, *disjointed,* as encoding the *Drosophila* Archease.

Although evolutionarily ancient, relatively few studies have focused on Archease (Canaves 2004, Auxilien, El Khadali et al. 2007, Desai, Cheng et al. 2014, Jurkin, Henkel et al. 2014, Popow, Jurkin et al. 2014, Desai, Beltrame et al. 2015, Kosmaczewski, Han et al. 2015, Song, Sretavan et al. 2015, Poothong, Tirasophon et al. 2017, Duan, Gao et al. 2020). Compelling work has established a requirement for Archease as a cofactor for the RNA ligase, RtcB (Popow, Jurkin et al. 2014). Together, Archease and RtcB play an essential role in transfer RNA (tRNA) maturation and in unconventional splicing of *X-box protein 1* (*Xbp1*) mRNA (Desai, Cheng et al. 2014, Jurkin, Henkel et al. 2014, Popow, Jurkin et al. 2014, Desai, Beltrame et al. 2015, Poothong, Tirasophon et al. 2017).

Nascent tRNAs undergo three processing events to become mature tRNAs ready to function in translation: 1) removal of the 3' extension sequences, 2) intron splicing and ligation and 3) aminoacylation. Archease and RtcB are required for the second of these tRNA maturation steps. Unlike mRNA splicing, tRNA splicing is not mediated by the spliceosome, but is instead carried out by complexes containing only protein. Not all tRNAs contain an intron, but throughout the animal kingdom roughly 6 to 7% of tRNA genes (slightly higher in zebrafish and frogs, and closer to ~ 25% in budding and fission yeast) contain an intron(Schmidt and Matera 2020). The tRNA splicing endonuclease (SEN/TSEN) complex initiates the splicing process by cleaving the tRNA intron (Schmidt and Matera 2020). Plants and fungi differ from metazoans in using a "healing and sealing" ligation pathway, rather than a direct ligation pathway (Schmidt and Matera 2020). The tRNA ligase complex consists of the core tRNA ligase (HSPC117/RtcB) and ASW (also known as C2orf49), CGI-99 (also known as C14orf166), FAM98B and the DEAD-box helicase, DDX1 (Kroupova, Ackle et al. 2021). Archease (ARCH, or ZBTB8OS) is a co-factor for RtcB and is required for full activity of the tRNA ligase(Popow, Jurkin et al. 2014); however, its interaction with RtcB is transient (Kroupova, Ackle et al. 2021). Unlike the "healing and sealing" pathway, the direct ligation pathway produces not only a spliced tRNA, but also a circular intronic RNA, tricRNA, of poorly understood function. In yeast, splicing of tRNAs occurs in the

cytoplasm, in association with mitochondria, while in eukaryotes, pre-tRNA splicing occurs in the nucleoplasm (reviewed in (Chatterjee, Nostramo et al. 2018)).

The tRNA ligase complex and Archease also are required for the nonconventional splicing of a transcription factor in the cytoplasm (Jurkin, Henkel et al. 2014). Xbp1 is a transcription factor that induces a suite of unfolded protein response (UPR) genes under conditions of ER stress. In the absence of ER stress, *Xbp1* mRNA encodes for a nonfunctional protein, Xbp1m. Upon ER stress, the nuclease activity of the Inositol-requiring enzyme 1 (IRE1) stress sensor is activated, and cleaves the *Xbp1* mRNA. The mRNA fragments are then ligated by Archease/RtcB (Jurkin, Henkel et al. 2014), resulting in a change in the reading frame of the transcript, and consequent translation of a functional Xbp1s transcription factor. Nonconventional splicing of the *Xbp1* mRNA is thought to be cytoplasmic, as the mRNA is localized to the ER membrane, where IRE1 cleaves it to initiate nonconventional splicing ((Back, Lee et al. 2006, Uemura, Oku et al. 2009, Yanagitani, Imagawa et al. 2009, Wang, Xing et al. 2015) but also see (Wang, Xing et al. 2015)).

Taken together, requirements for RtcB/Archease at the cytoplasmic face of the ER, and in the nucleus, implies that the tRNA ligase complex/Archease can shuttle between the nucleus and the cytoplasm. Indeed, the tRNA ligation complex is known to shuttle, and has been found both in the nucleus and in association with cytoplasmic RNA granules(Perez-Gonzalez, Pazo et al. 2014, Duan, Gao et al. 2020). Published data have described a broad cytoplasmic distribution of Archease, at least in cell culture (Jurkin, Henkel et al. 2014, Duan, Gao et al. 2020). Here we characterize the requirement for Archease in tracheal terminal cell morphogenesis, identify a primarily nuclear localization for Archease, and uncover regulation of Archease subcellular localization by Tor-vATPase pathway activity.

RESULTS

Terminal cells mutant for *disjointed* show a gap in gas-filling

A gap in gas-filling at the stalk cell:terminal cell interface is characteristic of a group of mutations – *oak gall (okg)*, *conjoined (cnj), lotus*, and *disjointed* – that we first identified in a forward genetic screen (Ghabrial, Levi et al. 2011). While mutations in *okg* and *cnj* were found to cause a gas-filling gap in terminal cells due to invasion by neighboring wild type stalk cells, mutations in *lotus* disrupted the connection between seamed and seamless tubes in the terminal cell(Song, Eng et al. 2013, Francis and Ghabrial 2015). We determined that *lotus* encodes Nsf2, and is therefore required for vesicle trafficking, while *okg* and *cnj* each encode a subunit of the vacuolar ATPase, and were determined to act downstream of Tor in regulating apical membrane domain size. We chose to further characterize the single mutant allele of *disjointed* (*dsj)*, the last remaining member of this phenotypic class (**Figure 1A,B**). We found that in addition to the transition zone gas-filling defects (59% of terminal cells), 24% of *dsj* terminal cells entirely lacked gas-filling while 17% were normally gas-filled (n=41). Examination of terminal cell tubes revealed that they are continuous (like *okg* and *cnj* mutants).

Terminal cells mutant for *disjointed* induce neighboring stalk cell branching and hypertrophy

Given their striking phenotypic similarity, we next asked if *disjointed* mutant terminal cells induced compensatory stalk cell branching, similar to that documented for cells mutant for members of the Tor-vATPase axis *(Francis and Ghabrial 2015)*. In wild type animals, terminal cells connect to neighboring stalk cells at a single intercellular connection 96% of the time (**Figure 1C**) while 4% made two connections to the same terminal cell. The intercellular connection includes septate (functionally equivalent to vertebrate tight junctions for paracellular barrier function) and adherens junctions. Consistent with the phenotype previously described for mutants in the TOR-vATPase axis(Francis and Ghabrial 2015), in *dsj* mosaic animals, 72% (n=54) of mutant terminal cells had two connections to their neighboring stalk cell, while an additional 4% of *dsj* terminal cells were invaded by long extensions of stalk cell auto-cellular tube terminating in 3 or more intercellular connections (**Figure 1C-E**).

disjointed^{169} carries a missense mutation in the Archease coding sequence

To better understand the cell biological and molecular functions of *dsj* in the context of the terminal cell-to-stalk cell interface, we mapped the mutation (**Figure 2A**). Sequence analysis of candidate genes within the candidate interval revealed a G to A transition in the third exon of the gene, *CG6353*, which encodes the *Drosophila* orthologue of human Archease/ZBTB8OS (**Figure 2B**). This missense mutation is predicted to convert a highly conserved glycine residue to glutamic acid, creating a loss of function allele ($G_{115}E$). Archease proteins across kingdoms have been implicated in DNA or RNA metabolism (Auxilien, El Khadali et al. 2007, Desai, Cheng et al. 2014), with more recent work identifying Archease as a cofactor for RtcB, an RNA ligase required for transfer RNA (tRNA) maturation and nonconventional splicing of *X Box protein 1* (*Xbp1*) mRNA (Desai, Cheng et al. 2014, Popow, Jurkin et al. 2014).

Two additional experiments confirmed gene identity. Expression of an inducible wild type *Archease* cDNA construct rescued terminal cell gas-filling and morphology in *dsj* mutant cells (**Figure 2C**), while depletion of *CG6353* by RNAi in otherwise wild type larvae reproduced the defects observed in *dsj* mutant terminal cells (**Figure 2D**). Terminal cell-specific depletion of *CG6353* resulted in a substantial increase in the number of terminal cells connected to neighboring stalk cells by two intercellular junctions (43%, n=76), and resulted in a striking number of terminal cells (37%) invaded by three or more autocellular tubes (a condition which has never been observed at all in wild type). The increased frequency of the more severe phenotype upon *dsj* knockdown, as compared to the *dsj* point mutation, suggests the existence of maternally deposited *dsj* mRNA, or that the point mutation in *dsj* is hypomorphic, or both. Consistent with maternal deposition of Archease, *dsj* homozygous animals survive until the 2nd larval instar; however, we could not further test this hypothesis as maternal depletion of *dsj* resulted in defective oogenesis (data not shown). Taken together, these data establish that *dsj* encodes Archease.

Archease localizes to tracheal cell nuclei

The rescuing transgene we generated was N-terminally tagged with the HA epitope. Although, we were unable to identify a canonical nuclear localization signal in Archease, we observed strong nuclear localization of tagged Archease in rescued tracheal cells (**Figure 3A**, **A'**). While this result was consistent with a requirement for Archease in tRNA maturation (which occurs in the nucleus), it conflicts with previously published data from (HeLa) cells suggesting an exclusively, or largely, cytoplasmic localization for Archease (Jurkin, Henkel et al. 2014, Duan, Gao et al. 2020).

Mutations in vATPase and Rheb result in loss of Archease from terminal cell nuclei

Since *dsj* displays phenotypes similar to *okg* and *cnj* (which encode two vATPase subunits), we sought to determine whether v-ATPase activity regulates *dsj*. We found that, in contrast to a robust nuclear signal in wild type terminal cells, Archease was absent from *cnj/vha13* terminal cell nuclei (**Figure 3B**, yellow arrowhead) and instead accumulated in the cytoplasm. In internal controls, (neighboring heterozygous cells in the same larvae), Archease remained nuclear (**Figure 3B, white arrowheads**). We and others have reported that the vATPase acts genetically downstream of the Tor pathway(Gleixner, Canaud et al. 2014, Francis and Ghabrial 2015). Since, Archease regulates tRNA maturation, which is necessary for protein synthesis, we sought to determine whether Tor pathway activity was required for Archease localization to the nucleus. To this end, we generated *Rheb* mosaic animals and examined the homozygous mutant terminal cells. Although, some Archease was still localized to the small Rheb terminal cell nuclei, a very substantial shift to the cytoplasm was detected (**Figure 3C**); in particular, as compared to neighboring internal control heterozygous cells (white arrowheads). This suggested that activity of the Tor- vATPase axis drives Archease to the nucleus, or is required for its maintenance there. Genetic epistasis tests of *Archease/disjointed* loss of function with *TSC1/jolly green giant* loss of function, or with over-expressed Rheb, are consistent with *Archease/disjointed* acting downstream of TOR (Figure S1).

Disruption of tRNA maturation induces stalk cell compensatory branching.

Archease acts as a co-factor for tRNA ligase RtcB (Popow, Jurkin et al. 2014) during one step of tRNA maturation, a multi-step process that begins with intron splicing and 3' end ligation, followed by 5' and 3' end processing (Yoshihisa 2014). The 3' ends are removed by the endoribonuclease tRNAse Z (the *Drosophila* homologue of human ELAC1/2) (Takaku, Minagawa et al. 2003). Removal of the 5' and 3' ends is followed by the addition of CCA, which prepares tRNAs for aminoacylation and nuclear export (Hopper and Shaheen 2008). To test whether defects associated with loss of *dsj* could result from its role in tRNA processing, we depleted *tRNAseZ* from terminal cells and assessed the intercellular junction phenotype. We observed that 68% (N=47) of *tRNAseZ* depleted terminal cells displayed stalk cell invasion defects (**Figure 4**). Similar results obtained from blocking nuclear export of RNAs, including tRNAs, by knockdown of NTF2-related export protein 1 *(NXT1)*: terminal cells were recovered with 2 intercellular junctions (43%) and with 3 or more intercellular junctions (26%) (n=46).

Loss of Xbp1 function does not affect tracheal terminal cell morphology

To test whether the loss of non-convential splicing of *Xbp1* could also phenocopy the terminal cell requirement for Archease, we depleted cells of *Xbp1* mRNA by RNAi and also examined trachea of larvae null for *Xbp1*, but rescued to viability by *Xbp1* cDNA expression in the alimentary canal (Huang, Zeng et al. 2017). Prior studies have established that *Xbp1s* nonconventional splicing occurs at detectable levels in wild type larval trachea, brain glia, Malpighian tubules and gut, whereas *Xbp1s* splicing in other tissues appears to require induction of ER stress (Sone, Zeng et al. 2013). We found that loss of *Xbp1* did not perturb terminal cell development or morphology, consistent with the hypothesis that it is the requirement for Archease in tRNA maturation that results in the *disjointed* phenotype.

DISCUSSION

In this and previous work(Francis and Ghabrial 2015, Burguete, Francis et al. 2019), we determined that most mutations that impair tracheal terminal cell apical membrane growth, and in particular, mutations in components of the TOR pathway, trigger induction of a compensatory growth program in neighboring wild type tracheal stalk cells. As part of this compensatory program, stalk cells, which form autocellular tubes, are induced to grow, branch, and extend into the terminal cell. These two cells, which normally share a single intercellular junction, instead share two, three or more intercellular junctions. Moreover, these junctions are no longer located at the initial point of cell-cell contact, but instead, the stalk autocellular tubes and their surrounding cytoplasm invade the terminal cell and become enveloped by the cytoplasm of the terminal cell. One fascinating and unresolved question is whether this invasion of the terminal cell requires the generation of a signal from the terminal cell to the stalk cell, or whether the altered mechanical properties of the terminal cell are sufficient to trigger compensatory growth.

The relationship between core TOR pathway components, the vATPase, and Archease is complex. In our prior work (Francis and Ghabrial 2015), we determined that vATPase is epistatic (downstream) to TOR in regulating apical membrane growth, consistent with the results of Gleixner and colleagues (Gleixner, Canaud et al. 2014). However, the genetic relationships are not quite so straightforward, as vATPase activity also regulates mTOR(Pena-Llopis, Vega-Rubin-de-Celis et al. 2011, Zoncu, Bar-Peled et al. 2011). There had been no previous indication in the literature that TOR would regulate Archease; however, given TOR's role in promoting translation, and Archease's role in tRNA splicing, such regulation has an appealing logic.

We found that mutations in *Rheb* as well as vATPase components *oakgall/Vha26* and *conjoined/Vha13* had profound effects on Archease subcellular localization. In wild type tracheal cells, Archease appeared greatly enriched in nuclei – we found this distribution of Archease in *Drosophila* to be consistent across multiple tissues including salivary gland epithelia and neurons (data not shown). This stands in contrast to published

reports of Archease localization in HeLa cells (Jurkin, Henkel et al. 2014, Duan, Gao et al. 2020), where Archease is reported to be largely cytoplasmic. This difference may reflect differences between post mitotic and actively cycling cells, cells in culture as compared to in vivo, or other factors. Importantly, in *vATPase* and *Rheb* mutant cells, there was a dramatic redistribution of Archease from the nucleus to the cytoplasm. The subcellular localization of Archease is likely important, as its two best characterized functions, splicing of tRNA introns and splicing of Xbp1 mRNA, are thought to occur in the nucleus and the cytoplasm, respectively. This would suggest that conditions required for induction of the stress response by Xbp1s might correspond with a general decrease in tRNA availability, and likewise, that robust mTOR driven cell growth might limit the ability of the cell to generate the Xbp1s isoform. A less well characterized role of the tRNA ligase complex and Archease is in the production of tricRNAs – circularized tRNA introns that are quite stable and abundant, but of unknown function (Schmidt and Matera 2020). A role for tricRNAs in compensatory growth cannot be ruled out.

In addition to implications for cellular growth and in stress response, regulation of Archease subcellular localization may also be of interest from the perspective of neuronal regeneration. Genetic disruption of the XBP1 arm of the UPR impedes axonal regeneration (Song, Sretavan et al. 2015, Onate, Catenaccio et al. 2016) (although also see (Kosmaczewski, Han et al. 2015)). This would suggest that cytoplasmic localization of Archease, where it would be required for productive splicing of *xbp1* mRNA, might contribute to regeneration. However, the depletion of the mTOR pathway inhibitors, PTEN and Tuberous Sclerosis 1/Hamartin (Tsc1), significantly enhances axonal regeneration(Park, Liu et al. 2008, Liu, Lu et al. 2010, Park, Liu et al. 2010, Song, Ori-McKenney et al. 2012, Yang, Miao et al. 2014, Du, Zheng et al. 2015, Miao, Yang et al. 2016), and would be predicted to shift Archease to the nucleus. It may be that under these conditions sufficient Archease is present in the cytoplasm to promote *xbp1* splicing, or, alternatively, it may be that regeneration could be further enhanced by upregulation of Archease expression together with activation of Tor signaling.

MATERIALS AND METHODS

Fly stocks:

btl-Gal4, UAS-DsRED2^{NLS}, UAS-GFP; FRT^{82B} UAS-*GFP* RNAi

btl-GAL4, UAS-GFP; FRT^{2A}, FRT^{82B} *dsj*^{169}/ TM3, Sb, Tub-GAL80 (Ghabrial et al., 2011)

btl-GAL4, UAS-GFP; FRT^{2A}, FRT ^{82B} *TSC1* ^{jollygreengiant} /TM3, Sb, Tub-GAL80 (Ghabrial et al., 2011)

FRT^{82B} *cnj* ^{356}/ TM6 (Francis and Ghabrial, 2015)

SRF>GAL4 (gift of M.Metzstein, Utah),

P{TRiP.HMS03015}attP2 – xbp1 RNAi (Bloomington Bloomington *Drosophila* Stock Center)

P{TRiP.JF02012}attP2– xbp1 RNAi (Bloomington Bloomington *Drosophila* Stock Center)

UAS-*CG6353* ^{HMS02543} (*dsj*) RNAi (Bloomington *Drosophila* Stock Center)

UAS-*Rheb*^{PA} (Bloomington *Drosophila* Stock Center)

UAS-*tRNAse Z* $^{jhl\text{-}1\ HMC03826}$ RNAi (Bloomington *Drosophila* Stock Center)

UAS-*NXT1* ^{GL00414} RNAi (Bloomington *Drosophila* Stock Center)

TRiP JF02012 (Xbp1 RNAi) (Song, Sretavan et al. 2015) (Bloomington *Drosophila* Stock Center)

4E-BP^{intron} *DsRed*, *Xbp1*^{ex79}*; UAS-Xbp1-RA/SM5-TM6B* were crossed with *NP1-GAL4, Xbp1*^{ex79}*/CyO,GFP; tho2p>DsRed/*TM6B to produce *Xbp1* null larvae rescued to viability by *BP1>xbp1* (gifts from Ron Ryoo). 10 dorsal branch terminal cells from each of 5 animals of the correct genotype were examined.

Immunoflourescence: 3rd instar larvae of both genders were filleted and fixed in 4% PFA (EMS) for 15 minutes at room temperature. Antibodies used: Rat anti-DE-Cadherin (1:50, DSHB), Rb anti-aPKC (PKCz, 1:200, Santa Cruz), Chk anti-GFP (1:1,000, Invitrogen A10262), Mouse anti-HA tag (1:100, Clone HA7, Sigma H3663). Larvae were mounted in aqua polymount (Polysciences), and images were acquired on Leica DM5500 and DMI6000 B microscopes. Z stacks were captured and processed with Leica and Fiji (imageJ) software. Projected z stacks or single slices are shown, as noted. Statistical significance was determined using the fisher exact probability test (www.vasserstats.net)

Rescue construct:

Generation of pUASt–HA-*dsj*: *CG6353* complementary DNA FI17516 (DGRC) was used as a template for PCR primers. A PCR product containing an N-terminal HA tag was sub-cloned into pUAST (Brand and Perrimon 1993). The transgene was injected into w^{1118} embryos to generate UAS-HA-*dsj* transgenic flies.

RNAi knockdown studies

SRF-GAL4 or *drm*-GAL4 driven expression of UAS-*CG6353* ^{HMS02543} RNAi , UAS-tRNAse Z $^{jhl\text{-}1\ HMC03826}$ RNAi, UAS-*NXT1* ^{GL00414} RNAi, and UAS-GFP. Flies were kept at 29 degrees and 3rd instar larvae were collected.

Transgene rescue of dsj TCs:

The following crosses were carried out:

UAS-HA-dsj; FRT^{82B} dsj^{169} /TM6B flies were crossed to *btl*-GAL4, UAS-RFP/CyO; FRT^{82B} Tubulin Gal80 /TM6B. Mosaic larvae with RFP marked clones were collected for immunostaining.

Sequence analyses:

dsj genomic DNA and control genomic DNA from the parental strain on which *dsj* mutations were induced, were amplified by PCR and sequenced. The following primers were used: *CG6353* genomic region

F1 5'- GCATAGATGGTCACACTAAGCGG -3'

R1 5'- AAATCGCTCGGTGTTACCAGC -3'

F2 5'- TCAGTAGGGAGAACTTCCTGCTGC -3'

R2 5'- TGGATTCTGTCAAATGGGAAGG -3'

F3 5'- CAAAAACAACAAGTGTGCCCG -3'

R3 5'- ATTGCCTTCACTTCGGTGCC -3'

F4 5'- TGTGACTGTTCTGTTTCAACCCC -3'

Epistasis Experiments:

The following crosses were carried out:

UAS-*Rheb* (homozygous on the 2nd), FRT ^{82B} *dsj* / TM6 males were crossed to *btl*>Gal4, UAS-*GFP*, FRT ^{82B} UAS-*GFP* RNAi females to generate clones. Junction phenotypes of GFP marked terminal cells were compared to unmarked terminal cells within the same larvae.

UAS-*CG6353* ^{HMS02543} RNAi (homozygous on 2nd), FRT ^{82B} *TSC1*^{jollygreengiant}/TM3 males were crossed to *btl*>Gal4, UAS-*GFP*, FRT ^{82B} UAS-*GFP* RNAi females. Mosaic larvae were collected, filleted, immunostained and imaged.

Acknowledgements

Some of the text and data in this paper formed a part of Deanne Francis's PhD thesis in the Department of Cell and Developmental Biology at the University of Pennsylvania in 2015. This research was supported by NIH GRANT R01 GM089782 to ASG. Stocks obtained from the Bloomington *Drosophila* Stock Center (NIH P40OD018537) were used in this study.

REFERENCES

Auxilien, S., F. El Khadali, A. Rasmussen, S. Douthwaite and H. Grosjean (2007). "Archease from Pyrococcus abyssi improves substrate specificity and solubility of a tRNA m5C methyltransferase." J Biol Chem **282**(26): 18711-18721.

Back, S. H., K. Lee, E. Vink and R. J. Kaufman (2006). "Cytoplasmic IRE1alpha-mediated XBP1 mRNA splicing in the absence of nuclear processing and endoplasmic reticulum stress." J Biol Chem **281**(27): 18691-18706.

Brand, A. H. and N. Perrimon (1993). "Targeted gene expression as a means of altering cell fates and generating dominant phenotypes." Development **118**(2): 401-415.

Burguete, A. S., D. Francis, J. Rosa and A. Ghabrial (2019). "The regulation of cell size and branch complexity in the terminal cells of the Drosophila tracheal system." Dev Biol.

Canaves, J. M. (2004). "Predicted role for the archease protein family based on structural and sequence analysis of TM1083 and MTH1598, two proteins structurally characterized through structural genomics efforts." Proteins **56**(1): 19-27.

Caussinus, E., J. Colombelli and M. Affolter (2008). "Tip-cell migration controls stalk-cell intercalation during Drosophila tracheal tube elongation." Curr Biol **18**(22): 1727-1734.

Chatterjee, K., R. T. Nostramo, Y. Wan and A. K. Hopper (2018). "tRNA dynamics between the nucleus, cytoplasm and mitochondrial surface: Location, location, location." Biochim Biophys Acta Gene Regul Mech **1861**(4): 373-386.

Desai, K. K., A. L. Beltrame and R. T. Raines (2015). "Coevolution of RtcB and Archease created a multiple-turnover RNA ligase." RNA **21**(11): 1866-1872.

Desai, K. K., C. L. Cheng, C. A. Bingman, G. N. Phillips, Jr. and R. T. Raines (2014). "A tRNA splicing operon: Archease endows RtcB with dual GTP/ATP cofactor specificity and accelerates RNA ligation." Nucleic Acids Res **42**(6): 3931-3942.

Du, K., S. Zheng, Q. Zhang, S. Li, X. Gao, J. Wang, L. Jiang and K. Liu (2015). "Pten Deletion Promotes Regrowth of Corticospinal Tract Axons 1 Year after Spinal Cord Injury." J Neurosci **35**(26): 9754-9763.
Duan, S., W. Gao, Z. Chen, Z. Li, S. Li, J. Gan, X. Chen and J. Li (2020). "Crystal structure of human archease, a key cofactor of tRNA splicing ligase complex." Int J Biochem Cell Biol **122**: 105744.

Francis, D. and A. S. Ghabrial (2015). "Compensatory branching morphogenesis of stalk cells in the Drosophila trachea." Development **142**(11): 2048-2057.

Ghabrial, A., S. Luschnig, M. M. Metzstein and M. A. Krasnow (2003). "Branching morphogenesis of the Drosophila tracheal system." Annu Rev Cell Dev Biol **19**: 623-647.

Ghabrial, A. S. and M. A. Krasnow (2006). "Social interactions among epithelial cells during tracheal branching morphogenesis." Nature **441**(7094): 746-749.

Ghabrial, A. S., B. P. Levi and M. A. Krasnow (2011). "A systematic screen for tube morphogenesis and branching genes in the Drosophila tracheal system." PLoS Genet **7**(7): e1002087.

Gleixner, E. M., G. Canaud, T. Hermle, M. C. Guida, O. Kretz, M. Helmstadter, T. B. Huber, S. Eimer, F. Terzi and M. Simons (2014). "V-ATPase/mTOR signaling regulates megalin-mediated apical endocytosis." Cell Rep **8**(1): 10-19.

Hopper, A. K. and H. H. Shaheen (2008). "A decade of surprises for tRNA nuclear-cytoplasmic dynamics." Trends Cell Biol **18**(3): 98-104.

Huang, H. W., X. Zeng, T. Rhim, D. Ron and H. D. Ryoo (2017). "The requirement of IRE1 and XBP1 in resolving physiological stress during Drosophila development." J Cell Sci **130**(18): 3040-3049.

Jurkin, J., T. Henkel, A. F. Nielsen, M. Minnich, J. Popow, T. Kaufmann, K. Heindl, T. Hoffmann, M. Busslinger and J. Martinez (2014). "The mammalian tRNA ligase complex mediates splicing of XBP1 mRNA and controls antibody secretion in plasma cells." EMBO J **33**(24): 2922-2936.

Kosmaczewski, S. G., S. M. Han, B. Han, B. Irving Meyer, H. S. Baig, W. Athar, A. T. Lin-Moore, M. R. Koelle and M. Hammarlund (2015). "RNA ligation in neurons by RtcB inhibits axon regeneration." Proc Natl Acad Sci U S A **112**(27): 8451-8456.

Kroupova, A., F. Ackle, I. Asanovic, S. Weitzer, F. M. Boneberg, M. Faini, A. Leitner, A. Chui, R. Aebersold, J. Martinez and M. Jinek (2021). "Molecular architecture of the human tRNA ligase complex." Elife **10**.
Liu, K., Y. Lu, J. K. Lee, R. Samara, R. Willenberg, I. Sears-Kraxberger, A. Tedeschi, K. K. Park, D. Jin, B. Cai, B. Xu, L. Connolly, O. Steward, B. Zheng and Z. He (2010). "PTEN deletion enhances the regenerative ability of adult corticospinal neurons." Nat Neurosci **13**(9): 1075-1081.

Manning, G. a. K., M.A. (1993). Development of the Drosophila tracheal system. The Development of Drosophila melanogaster. M. a. M. A. Bate, A. U.S.A., Cold Spring Harbor Laboratory Press. **I:** 609-686.

Miao, L., L. Yang, H. Huang, F. Liang, C. Ling and Y. Hu (2016). "mTORC1 is necessary but mTORC2 and GSK3beta are inhibitory for AKT3-induced axon regeneration in the central nervous system." Elife **5**: e14908.

Onate, M., A. Catenaccio, G. Martinez, D. Armentano, G. Parsons, B. Kerr, C. Hetz and F. A. Court (2016). "Activation of the unfolded protein response promotes axonal regeneration after peripheral nerve injury." Sci Rep **6**: 21709.

Park, K. K., K. Liu, Y. Hu, J. L. Kanter and Z. He (2010). "PTEN/mTOR and axon regeneration." Exp Neurol **223**(1): 45-50.

Park, K. K., K. Liu, Y. Hu, P. D. Smith, C. Wang, B. Cai, B. Xu, L. Connolly, I. Kramvis, M. Sahin and Z. He (2008). "Promoting axon regeneration in the adult CNS by modulation of the PTEN/mTOR pathway." Science **322**(5903): 963-966.

Pena-Llopis, S., S. Vega-Rubin-de-Celis, J. C. Schwartz, N. C. Wolff, T. A. Tran, L. Zou, X. J. Xie, D. R. Corey and J. Brugarolas (2011). "Regulation of TFEB and V-ATPases by mTORC1." EMBO J **30**(16): 3242-3258.

Perez-Gonzalez, A., A. Pazo, R. Navajas, S. Ciordia, A. Rodriguez-Frandsen and A. Nieto (2014). "hCLE/C14orf166 associates with DDX1-HSPC117-FAM98B in a novel transcription-dependent shuttling RNA-transporting complex." PLoS One **9**(3): e90957.

Poothong, J., W. Tirasophon and R. J. Kaufman (2017). "Functional analysis of the mammalian RNA ligase for IRE1 in the unfolded protein response." Biosci Rep **37**(2).

Popow, J., J. Jurkin, A. Schleiffer and J. Martinez (2014). "Analysis of orthologous groups reveals archease and DDX1 as tRNA splicing factors." Nature **511**(7507): 104-107.

Ribeiro, C., M. Neumann and M. Affolter (2004). "Genetic control of cell intercalation during tracheal morphogenesis in Drosophila." Curr Biol **14**(24): 2197-2207.

Samakovlis, C., N. Hacohen, G. Manning, D. C. Sutherland, K. Guillemin and M. A. Krasnow (1996). "Development of the Drosophila tracheal system occurs by a series of morphologically distinct but genetically coupled branching events." Development **122**(5): 1395-1407.

Samakovlis, C., G. Manning, P. Steneberg, N. Hacohen, R. Cantera and M. A. Krasnow (1996). "Genetic control of epithelial tube fusion during Drosophila tracheal development." Development **122**(11): 3531-3536.

Schmidt, C. A. and A. G. Matera (2020). "tRNA introns: Presence, processing, and purpose." Wiley Interdiscip Rev RNA **11**(3): e1583.

Schottenfeld, J., Y. Song and A. S. Ghabrial (2010). "Tube continued: morphogenesis of the Drosophila tracheal system." Curr Opin Cell Biol **22**(5): 633-639.

Sone, M., X. Zeng, J. Larese and H. D. Ryoo (2013). "A modified UPR stress sensing system reveals a novel tissue distribution of IRE1/XBP1 activity during normal Drosophila development." Cell Stress Chaperones **18**(3): 307-319.

Song, Y., M. Eng and A. S. Ghabrial (2013). "Focal defects in single-celled tubes mutant for Cerebral cavernous malformation 3, GCKIII, or NSF2." Dev Cell **25**(5): 507-519.

Song, Y., K. M. Ori-McKenney, Y. Zheng, C. Han, L. Y. Jan and Y. N. Jan (2012). "Regeneration of Drosophila sensory neuron axons and dendrites is regulated by the Akt pathway involving Pten and microRNA bantam." Genes Dev **26**(14): 1612-1625.

Song, Y., D. Sretavan, E. A. Salegio, J. Berg, X. Huang, T. Cheng, X. Xiong, S. Meltzer, C. Han, T. T. Nguyen, J. C. Bresnahan, M. S. Beattie, L. Y. Jan and Y. N. Jan (2015). "Regulation of axon regeneration by the RNA repair and splicing pathway." Nat Neurosci **18**(6): 817-825.

Takaku, H., A. Minagawa, M. Takagi and M. Nashimoto (2003). "A candidate prostate cancer susceptibility gene encodes tRNA 3' processing endoribonuclease." Nucleic Acids Res **31**(9): 2272-2278.

Tsarouhas, V., K. A. Senti, S. A. Jayaram, K. Tiklova, J. Hemphala, J. Adler and C. Samakovlis (2007). "Sequential pulses of apical epithelial secretion and endocytosis drive airway maturation in Drosophila." Dev Cell **13**(2): 214-225.

Uemura, A., M. Oku, K. Mori and H. Yoshida (2009). "Unconventional splicing of XBP1 mRNA occurs in the cytoplasm during the mammalian unfolded protein response." J Cell Sci **122**(Pt 16): 2877-2886.

Wang, Y., P. Xing, W. Cui, W. Wang, Y. Cui, G. Ying, X. Wang and B. Li (2015). "Acute Endoplasmic Reticulum Stress-Independent Unconventional Splicing of XBP1 mRNA in the Nucleus of Mammalian Cells." Int J Mol Sci **16**(6): 13302-13321.

Yanagitani, K., Y. Imagawa, T. Iwawaki, A. Hosoda, M. Saito, Y. Kimata and K. Kohno (2009). "Cotranslational targeting of XBP1 protein to the membrane promotes cytoplasmic splicing of its own mRNA." Mol Cell **34**(2): 191-200.

Yang, L., L. Miao, F. Liang, H. Huang, X. Teng, S. Li, J. Nuriddinov, M. E. Selzer and Y. Hu (2014). "The mTORC1 effectors S6K1 and 4E-BP play different roles in CNS axon regeneration." Nat Commun **5**: 5416.

Yoshihisa, T. (2014). "Handling tRNA introns, archaeal way and eukaryotic way." Front Genet **5**: 213.

Zoncu, R., L. Bar-Peled, A. Efeyan, S. Wang, Y. Sancak and D. M. Sabatini (2011). "mTORC1 senses lysosomal amino acids through an inside-out mechanism that requires the vacuolar H(+)-ATPase." Science **334**(6056): 678-683.

Figures

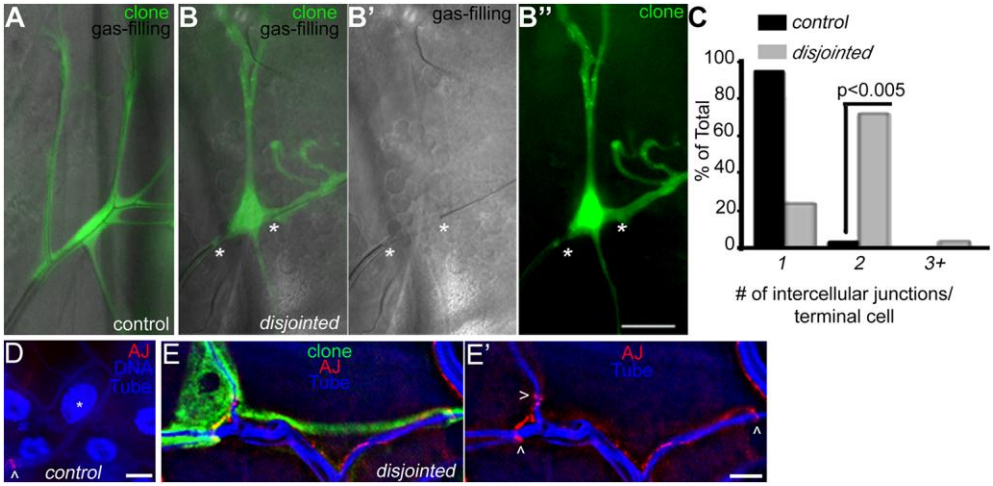

Fig. 1. Mutations in *dsj* cause gas-filling defects and stalk cell invasion. In (A), a control terminal cell clone is shown (green). The gas-filled tubes (revealed by bright-field microscopy) extend and branch throughout the terminal cell. In (B), a *disjointed* clone with a gap in gas-filling is shown (position of gap extends between *). The gas-filling defect is clearly visible by bright-field microscopy (B'); although fluorescence analysis (B'') reveals the presence of a GFP excluding lumen. Mosaic control and *disjointed* larvae were filleted and stained to reveal adherens junctions (β-Catenin). The number of intercellular junction per terminal cell clone was determined and is displayed in (C). A statistically significant enrichment in cells with two intercellular junctions was observed ($p<0.005$), while a few cells with 3 or more intercellular junctions were observed in disjointed clones but never in control. For control in C, 84 terminal cells were scored, for *dsj* terminal cell clones, 54 were scored. In (D and E), adherens junction (AJ) staining (α-DECadheren, red) is shown for terminal and stalk cells. Tubes are marked by autofluorescence in the UV channel (blue) and in (D), DAPI staining (also blue) marks DNA. The position of the intercellular junction is indicated by <. In (D), a single intercellular junction connects the control terminal cell (extending up and to the right, nucleus marked with *) and its neighboring stalk cell (see line of autocellular junctions extending to the left from the intercellular junction). In (E), the dsj terminal cell (green) makes three intercellular junctions with its neighboring stalk cell, which has branched and invaded the terminal cell. Statistical significance was determined by the Fischer exact probability test. Scale bars in B" (for A and B panels) = 10 microns. Scale bar in D = 10 microns, Scale bar in E' = 5 microns).

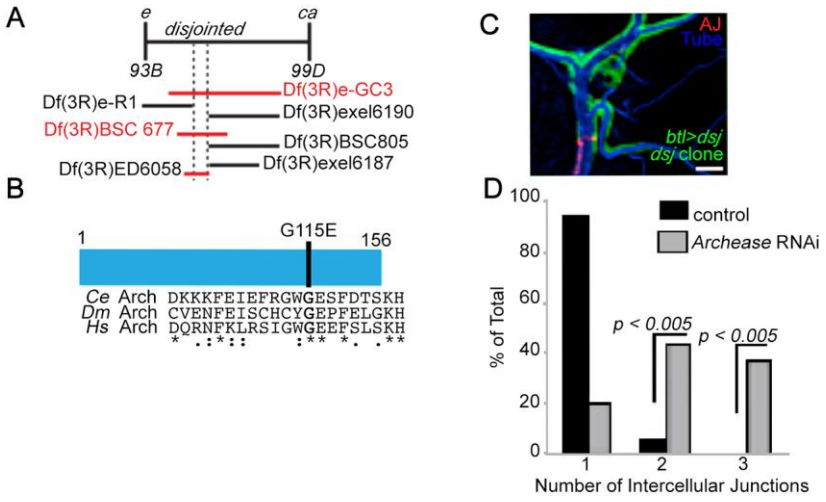

Fig. 2. *disjointed* encodes Archease. (A) *disjointed* was mapped to a region between the visible recessive markers *ebony (e)* and *claret (ca)* which map to polytene chromosome bands 93B and 99D, respectively. Overlapping chromosomal deletions spanning the interval were tested for complementation of *disjointed*. Deficiency mapping further refined a candidate region of 101.4 kbp – deficiency lines in red uncovered *disjointed* while those displayed in black, covered. Sequence analysis of genes in the candidate region identified a mis-sense mutation in Archease. In (B), a simple schematic of Archease is shown; the missense mutation in the 3rd exon of Archease (*CG6353*) is predicted to change a highly conserved glycine residue to a glutamic acid. An alignment of sequences from human, nematode and fly are shown, with the conserved glycine residue affected by the missense mutation indicated in bold. In (C), expression of a wild type *archease* cDNA was able to rescue the terminal cell gas-filling and tube invasion defects. Homozygous mutant *dsj* cell is marked by RFP expression (shown here as green) and co-expresses the rescuing wild type cDNA. Tubes (blue) are revealed by autofluorescence in the UV channel, and Adherens junction staining (AJ, red) was carried out using an antibody to DE-Cadheren. In (D), RNAi knockdown of Archease was scored and found to phenocopy *dsj* gas-filling (not shown) and cell junction defects, but with an increase in the severity of the phenotype. For control terminal cells, 70 were scored and for CG6353 RNAi, 76 terminal cells were scored. Scale bar in C = 10 microns.

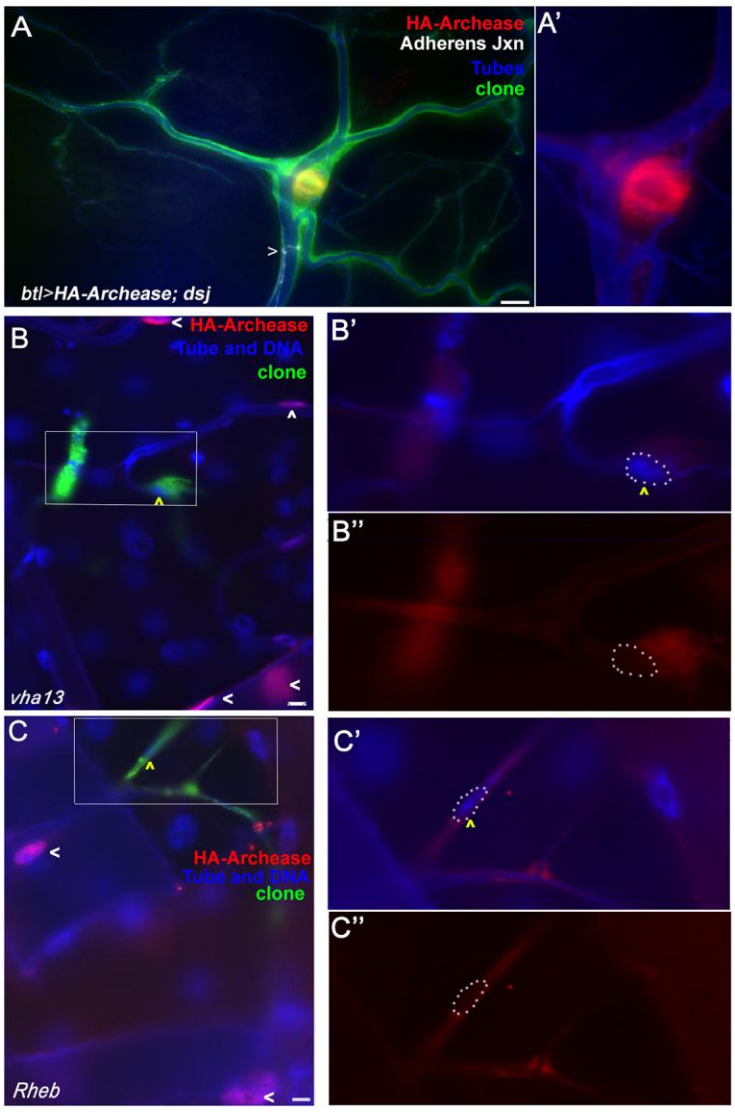

Fig. 3. Archease is localized to the nucleus in a TOR pathway-dependent manner. Max projections of deconvolved z stacks are shown. (**A)** In mosaic larvae, HA-tagged Archease (red) was localized to the nucleus of *disjointed/Archease* GFP positive mutant terminal cells (green). As in Figure 3, Archease expression was sufficient to rescue terminal cell morphology, suggesting HA-Archease is fully functional. The architecture of the stalk cell-terminal cell interface is also rescued, as indicated by the ring-like intercellular junction (adherens junction staining in white**,** intercellular junction (ring) indicated >). (B, C) GFP-labelled mutant cells (green) show altered Archease distribution. A single mutant cell is shown in each panel, but in (B) appears as two distinct regions of GFP positive cytoplasm due to neighboring stalk cell invasion. *Note there is a single terminal cell nucleus in each panel, indicated by yellow* ^. (**B**) A *vha13* mutant cell (green) is shown where HA-Archease (red) is cytoplasmic. Note HA-

Archease in neighboring heterozygous cells (white >) are nuclear – the larger red nucleus in the bottom right is from a dorsal trunk cell. Nuclei were labeled with DAPI (blue) and UV autofluorescence of tracheal tubes is also shown in blue. (B' and B'') show the area marquee by white rectangle at higher magnification. HA-Archease (red) is excluded from the terminal cell nucleus, indicated by yellow ^ (the dashed oval in magnified view outlines nucleus. DAPI (blue), stains the DNA but note that the tubes also autofluoresce in the UV channel. B' shows overlay of UV channel and HA-Archease, while B'' shows HA-Archease staining alone. (**C**) A *Rheb* mutant terminal cell (green) is shown. As expected, cell size is strongly impacted. As in *vha13* mutant cells, HA-Archease (red) is detected in the cytoplasm and largely excluded from the terminal cell nucleus in *Rheb* mutant terminal cells (DAPI as above in (B); yellow ^ indicates position of mutant terminal cell nucleus). Also note nuclear HA-Archease staining (red) in the neighboring heterozygous cells (white <). In (C' and C") the marqueed area in (C) is shown enlarged. (C') shows overlay of DAPI (DNA and tube autofluorescence) and HA-Archease staining (red). (C") shows HA-Archease staining alone. The position of the Rheb terminal cell nucleus is indicated by the white dotted oval. Elevated HA-Archease in the cytoplasm, as compared to the nucleus, is apparent. Images shown are representative, and at least 30 individual terminal cells of each genotype were imaged. Scale bars are 10 microns.

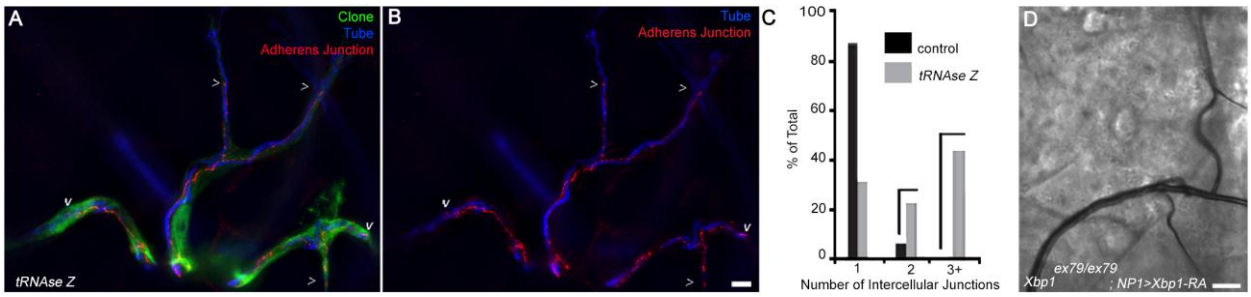

Fig. 4. Perturbing tRNA processing induces stalk cell invasion. In (A) terminal cell cytoplasm (*dSRF*>GFP, green), adherens junctions (β-catenin, red) and tube (UV autoflourescence, blue) of 3rd instar larva knocked down for tRNAse Z is shown. Arrowheads (>) indicate the position of intercellular junctions. In (B), the stalk cell invasion phenotype is quantified by scoring the number of intercellular junctions formed between a terminal cell and its stalk cell neighbor; control (black) and tRNAse Z RNAi (grey). In (C), *Xbp1* null larvae, rescued to viability by expression of an *Xbp1* cDNA exclusively in the alimentary canal, are shown to have grossly normal terminal cell morphology with no gas-filling defects. Statistical significance was determined by the Fischer exact probability test; $p < 0.005$. Scale Bar = 5μm.

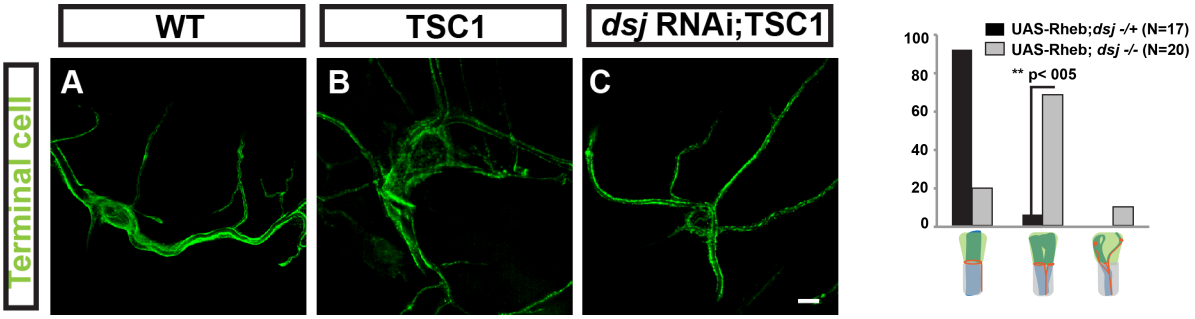

Fig. S1. Epistasis analysis suggests *dsj* acts genetically downstream of Tor. (A-C) Terminal cell (*btl*>GFP, green) are shown in 3rd instar larval fillets. (A) The cell soma and branches of a WT terminal cell are shown. (B) A TSC1 terminal cell has an enlarged soma, with increased branching, while depletion of *dsj* in TSC1 terminal cells were pruned and small(C). (D) Expression of UAS-*Rheb* did not suppress the *dsj* terminal cell junction defects. Statistical significance was determined by the Fischer exact probability test. Scale Bar 10 μm.